Contribution from the P. M. Gross Chemical Laboratory,
Department of Chemistry, Duke University, Durham, North Carolina 27706

Kinetics of Oxidation of a Cuprous 2,2',2''-Terpyridine Complex by Molecular Oxygen

ALVIN L. CRUMBLISS* and ARTHUR T. POULOS[1]

Received November 15, 1974 AIC40785W

2,2',2''-Terpyridine (terpy) has been found to form a bis cuprous complex, $Cu(terpy)_2^+$, in aqueous acetonitrile solution. The reaction with molecular oxygen was found to proceed with a two-electron reduction of O_2

$$2Cu(terpy)_2{}^+ + O_2 \xrightarrow{H^+} 2Cu(terpy)_2{}^{2+} + H_2O_2$$

The kinetics of this reaction has been studied at 25.0° over the pH range from 5.3 to 8.0, and the rate law found to be $-d[Cu(terpy)_2{}^+]/dt = k_{exptl}[Cu(terpy)_2{}^+][O_2]$, where $k_{exptl} = a + b[CH_3CN] + c[CH_3CN]^2/[terpy]_{xs}$, and $a = 1.6 \times 10^4\ M^{-1}\ sec^{-1}$, $b = 4.8 \times 10^3\ M^{-2}\ sec^{-1}$, $c = 5.1 \times 10^{-1}\ M^{-2}\ sec^{-1}$, and $[terpy]_{xs} = [terpy]_{tot} - 2[Cu^+]$. Possible mechanisms for this reaction are discussed.

Introduction

A study of the oxidation of cuprous complexes by molecular oxygen may enhance our understanding of the mechanism by which the copper-based oxygen transport system hemocyanin functions, as well as contribute to our understanding of the oxidation of transition metal ions by O_2.[2] The earliest report concerning the autoxidation of cuprous ion is that of Nord,[3] who studied the CuCl–HCl system using manometric techniques. More recently, Gray[4] and Zuberbühler[5] investigated the oxidation of aqueous cuprous ion in perchloric acid solutions containing acetonitrile. The rate of autoxidation of cuprous ion is found to be influenced by the ligand environment. Autoxidation kinetics have been reported for cuprous ion with carboxylic acids,[5] monodentate[6,7] and polydentate[8,9] nitrogen donor ligands, and mixed nitrogen–oxygen donor ligands.[8]

We report here on the kinetics of the reaction of a bis 2,2',2''-terpyridine[10] complex of copper(I) with molecular oxygen in aqueous solution containing acetonitrile. The presence of acetonitrile enhances the low solubility of terpy and thus allows a wider range of free ligand concentrations to be investigated. It also allows the use of $Cu(CH_3CN)_4ClO_4$[11,12] as a source of cuprous ions, which then precludes the necessity for cupric ion reducing agents which may interfere with the reaction of interest. The cuprous ion is stable to air oxidation for relatively long periods of time[4,5] in aqueous solutions containing from 2.0 to 4.5 M acetonitrile used in this study. This facilitated handling of the cuprous solutions and eliminated oxidation prior to terpy complex formation as a possible source of error in our measurements. The terpy ligand system was selected in order to study the influence of a potential tridentate nitrogen donor chelator with a π-electron system which would allow the cuprous ion readily to undergo a coordination number and geometry change upon oxidation with molecular oxygen.

Experimental Section

Materials. $Cu(CH_3CN)_4ClO_4$ was prepared and purified according to the method of Hemmerich and Sigwart.[12] The crystalline solid is stable and pure CH_3CN solutions stored in a dark refrigerator showed no decomposition over a period of months. The concentration of stock $Cu(CH_3CN)_4ClO_4$ solutions ($(3-4) \times 10^{-2}\ M$) in pure CH_3CN was determined by treatment with $6.0 \times 10^{-4}\ M$ 2,9-dimethyl-1,10-phenanthroline (neocuproine) in isoamyl alcohol, which had been fractionally distilled, and the absorbance at 454 nm recorded. The copper(I) concentration was calculated using the independently determined value $8.23 \times 10^3\ M^{-1}\ cm^{-1}$ for the molar extinction coefficient of $Cu(neocuproine)_2^+$ at 454 nm. The stock $Cu(CH_3CN)_4ClO_4$ did not contain any copper(II) species as the absorbance at 454 nm was not enhanced upon treatment with a 10% solution of $NH_2OH \cdot HCl$. $Cu(CH_3CN)_4ClO_4$ in aqueous CH_3CN (2.0–4.5 M used in this study) has an absorption maximum at 210 nm, ϵ $1.80 \times 10^4\ M^{-1}\ cm^{-1}$. $Cu(CH_3CN)_4ClO_4$ in aqueous solutions used in the kinetic studies described here, where $[CH_3CN] \geq 2.5\ M$, are stable to air oxidation over a period of hours. A small amount of decomposition with time was noted when $[CH_3CN] = 2.0\ M$. Copper(I) concentrations in the solutions used for kinetic runs were measured periodically during a series of kinetic experiments by measuring the absorbance of the $Cu(CH_3CN)_4ClO_4$ solution at 210 nm.

2,2',2''-Terpyridine (terpy) was obtained from the G. F. Smith Chemical Co. and recrystallized before use. All solutions except where noted otherwise were buffered using a $NaH_2PO_4 \cdot H_2O$–$NaHPO_4 \cdot 7H_2O$ buffer system. Some reactions incorporated a $HC_2H_3O_2$–$NaC_2H_3O_2$ buffer system to determine the possible influence of buffering ions on the reaction rate. Ionic strength variations were made using $NaClO_4$ as the inert electrolyte. No ionic strength influence on the rate was found over the range investigated up to $I = 0.7\ M$.

Methods. Electronic spectra were obtained in a N_2 atmosphere in solutions deoxygenated with prepurified N_2 gas using a Beckman Acta III spectrophotometer. Stock solutions of Cu^+ and terpy in deoxygenated aqueous CH_3CN were mixed under N_2 in an anaerobic spectrophotometric cell equipped with a threaded Teflon plug[13] using standard syringe techniques. $Cu(terpy)_2^+$ in 3.5 M aqueous CH_3CN has an absorption maximum in the visible region at 425 nm, ϵ $3.20 \times 10^3\ M^{-1}\ cm^{-1}$. Variations in CH_3CN concentrations from 2.0 to 4.5 M used in this study did not affect λ_{max} or ϵ.

The stoichiometry of the Cu^+ terpy complex was determined by the method of continuous variations.[14] terpy solutions prepared in 3.5 M CH_3CN containing pH 7.1 phosphate buffer with $I = 0.2\ M$ were degassed and added in 4-ml aliquots to an anaerobic spectrophotometric cell[13] and degassed further. The exact terpy concentration in each aliquot was determined spectrophotometrically at 290 nm where ϵ for terpy is $1.6 \times 10^4\ M^{-1}\ cm^{-1}$.[15] A 1-μl quantity of a freshly degassed stock solution of Cu^+ ($3.93 \times 10^{-2}\ M$) in pure CH_3CN such that $[Cu^+] + [terpy] = 8.0 \times 10^{-4}\ M$ was then added to the anaerobic cell and the absorbance at 425 nm measured at 25.0°. These results are shown in Figure 1.

A polarographic oxygen electrode (Beckman Instrument Co. Model 39065) connected to a Beckman Expandomatic pH meter (using a Beckman 96269 oxygen adapter for pH meters) was used to measure O_2 consumption by $Cu(terpy)_2^+$. A $2 \times 10^{-3}\ M$ air-saturated solution of the ligand in 3.5 M CH_3CN, pH 7.1 (phosphate buffer), was placed in a thermostated cell (25.0 ± 0.1°) of 13.4-ml dead volume containing a magnetic stirring bar and sealed with a Lucite cap containing the oxygen electrode. The O_2 concentration was determined from the millivolt display on the pH meter. Aliquots ranging from 0.03 to 0.2 ml of a stock $3.14 \times 10^{-2}\ M$ $Cu(CH_3CN)_4ClO_4$ in CH_3CN solution were then added through a small orifice in the Lucite cap while stirring. After the meter stabilized (ca. 1 min) the O_2 concentration was recorded from the millivolt display on the pH meter. The O_2 consumption was calculated from the difference in the two readings. The oxygen electrode was calibrated before and after each O_2 consumption measurement using air-saturated water at 25.0° ($2.62 \times 10^{-4}\ M$).[16] Calibration reproducibility before and after O_2 consumption measurements was ±1% of full scale.

The kinetics of the reaction of $Cu(terpy)_2^+$ with O_2 were monitored with a stopped-flow spectrophotometer at 425 nm where ϵ for $Cu(terpy)_2^+$ is $3.20 \times 10^3\ M^{-1}\ cm^{-1}$ and ϵ for $Cu(terpy)_2^{2+}$ is $7.1 \times 10^1\ M^{-1}\ cm^{-1}$. Selected kinetic experiments were also monitored at 730 nm where ϵ is 33 and 63 $M^{-1}\ cm^{-1}$ for $Cu(terpy)_2^+$ and $Cu(terpy)_2^{2+}$, respectively. These data collected at 730 nm were consistent with those collected at 425 nm, indicating that the rate of disappearance

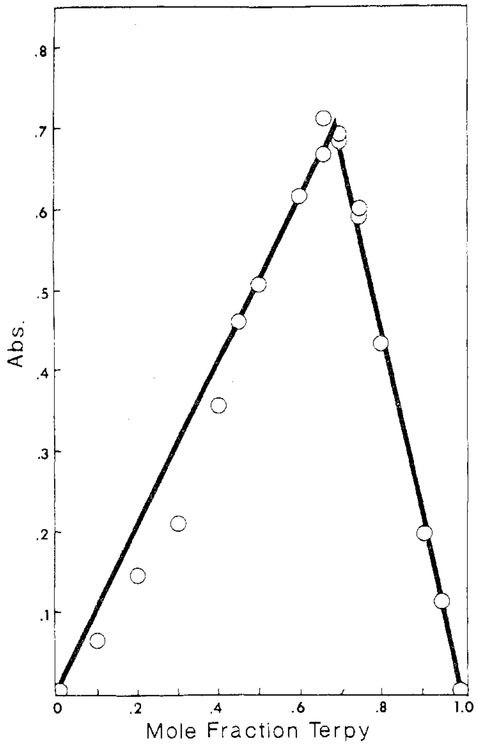

Figure 1. Anaerobic continuous-variations plot showing absorbance at 425 nm as a function of mole fraction of terpy. Conditions: $[\text{terpy}] + [\text{Cu}^+] = 8.0 \times 10^{-4}\ M$, $[\text{CH}_3\text{CN}] = 3.5\ M$, pH 7.1, $I = 0.2$, 25°, optical path length 1.0 cm.

of the cuprous complex is equal to the rate of formation of the cupric complex, as is required. All kinetic data reported in the text and figures were collected at 425 nm. A typical kinetic experiment was performed as follows. One drive syringe of the stopped-flow was charged with an aqueous solution containing appropriate concentrations of CH_3CN, $Cu(CH_3CN)_4ClO_4$, and O_2. (Solutions of $Cu(CH_3CN)_4ClO_4$ in 2.0–4.5 M CH_3CN used in this study are stable to air oxidation during the time of the experiment.) The other drive syringe was charged with an aqueous solution containing appropriate concentrations of CH_3CN, terpy, buffer, and O_2. The solutions were then allowed to come to thermal equilibrium prior to mixing. The formation of $Cu(terpy)_2{}^+$ was complete in time of mixing and not observed spectrophotometerically. The voltage vs. time curves corresponding to the oxidation of $Cu(terpy)_2{}^+$ by dissolved O_2 were recorded on a storage oscilloscope and photographed. Simultaneous with the kinetic experiments, the O_2 concentration of the copper and ligand solutions was determined using an oxygen electrode (see above), the pH of the reactant ligand and product solutions was measured, and the concentration of reactant copper solution was determined by measuring its absorbance at 210 nm on a Beckman Acta III recording spectrophotometer. The observed second-order rate constants, k_{exptl}, from eq 1 were calculated from the voltage vs. time photographs

$$\frac{-\text{d}[\text{Cu}^+]}{\text{d}t} = k_{\text{exptl}}[\text{Cu}^+][\text{O}_2] \tag{1}$$

according to eq 2 using a linear least-squares computer program and

$$\ln \frac{([\text{O}_2]_0 - {}^1\!/_2([\text{Cu}]_0 - [\text{Cu}^+]_t))}{[\text{Cu}^+]_t} = ([\text{O}_2]_0 - {}^1\!/_2[\text{Cu}^+]_0)k_{\text{exptl}} + \ln \frac{[\text{O}_2]_0}{[\text{Cu}^+]_0} \tag{2}$$

the Triangle Universities IBM 360-75 computer.

Results

Complex Stoichiometry and Spectra. The method of continuous variations[14] was used to determine the stoichiometry of the complex formed between copper(I) and terpy in aqueous CH_3CN. These data are presented in Figure 1 which shows a maximum at 0.69 mole fraction terpy, corresponding to a terpy:Cu^+ ratio of 2.2:1 and the stoichiometry of the complex as $Cu(terpy)_2{}^+$. The data shown in Figure 1 were obtained from solutions buffered at pH 7.1 with phosphate buffer. Data obtained under similar conditions without the addition of a buffer gave similar results, indicating that the presence of a phosphate buffer does not alter complex formation.

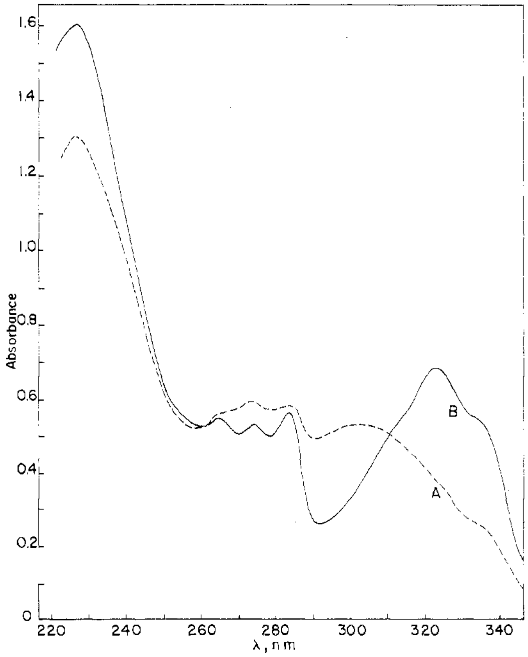

Figure 2. A. Anaerobic ultraviolet spectrum of $Cu(terpy)_2{}^+$. Conditions: $[\text{Cu}^+] = 1.7 \times 10^{-5}\ M$, $[\text{terpy}] = 3.8 \times 10^{-5}\ M$, $[\text{CH}_3\text{CN}] = 3.5\ M$, pH 6.9, optical path length 1.0 cm. B. Ultraviolet spectrum of solution A after exposure to O_2.

The anaerobic visible spectrum of $Cu(terpy)_2{}^+$ in aqueous CH_3CN has a characteristic absorption band at 425 nm (ϵ 3.20 × 10^3 M^{-1} cm^{-1}). Exposure of a solution of $Cu(terpy)_2{}^+$ to air results in a rapid oxidation to $Cu(terpy)_2{}^{2+}$, as indicated by an absorption maximum at 680 nm (ϵ 76 M^{-1} cm^{-1}), which corresponds to the visible spectrum of an authentic $Cu(terpy)_2{}^{2+}$ sample and is characteristic of the cupric complex.[17]

Figure 2 shows the ultraviolet spectrum of the oxidized and reduced form of the complex, which is dominated by absorptions due to electronic transitions centered on the terpy ligand. A considerable amount of structural information can be obtained from these spectra. Before discussing the spectra in Figure 2 in detail, it is useful to consider the spectrum of the pure ligand. terpy can exist in three configurations in aqueous solution, trans,trans, cis,trans, and cis,cis. The differences in configurations result from rotation about the C–C bond connecting α carbon atoms in the pyridine rings. Nakamoto[15] reported that in basic solution terpy exists in the trans,trans configuration and exhibits two absorption maxima at 290 and 227 nm. In solutions of intermediate pH three absorption maxima are clearly discernible at 320, 279, and 232 nm. A blurring of the fine structure in the 279-nm peak suggests rotation about the C–C bond. In acidic solution the cis,cis configuration predominates and fine structure in the 279-nm absorption band is evident, indicating a coplanar structure. Nakamoto[15] reported that metal complexes of terpy exhibit spectra similar to that of the free ligand in acidic solution. For example, [Zn(terpy)Cl]Cl has absorption maxima at 325, 285, and 230 nm; other metal complexes exhibit three absorption maxima in the ranges 340–320, 285–270, and 235–220 nm and exhibit fine structure. Independent evidence indicates that terpy is acting as a tridentate chelator in these systems and is in a planar cis,cis configuration.

Figure 2 shows three absorption maxima for $Cu(terpy)_2{}^+$

at 308, 275, and 227 nm, suggesting either a cis,trans or cis,cis configuration for the terpy ligand. The blurred fine structure seen in the broad absorption centered at 275 nm suggests free rotation about one of the C–C bonds connecting the pyridine rings. The most likely structure for $\mathrm{Cu(terpy)_2}^+$ appears to be I where terpy is acting as a bidentate ligand and one pyridine ring is left free to rotate in solution, i.e., a cis,trans terpy configuration. Oxidation to $\mathrm{Cu(terpy)_2}^{2+}$ results in an absorption spectrum with three maxima centered at 323, 275, and 227 nm and fine structure clearly discernible in the broad absorption centered at 275 nm. This is consistent with a planar cis,cis terpy configuration and suggests II as the solution structure for the $\mathrm{Cu(terpy)_2}^{2+}$ ion, in which terpy is acting as a tridentate ligand.

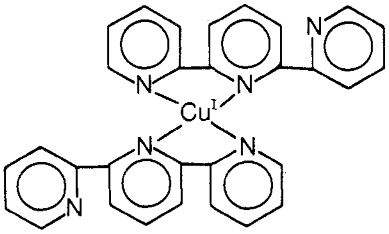

I

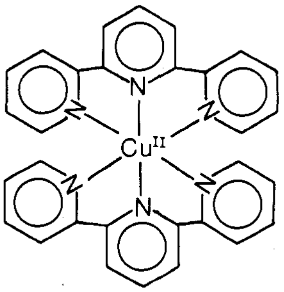

II

Reaction Stoichiometry. The overall stoichiometry of the reaction of $\mathrm{Cu(terpy)_2}^+$ with $\mathrm{O_2}$ has been determined using a polarographic oxygen electrode to measure changes in $\mathrm{O_2}$ concentration in a closed system (see Experimental Section). The ratio at which $\mathrm{Cu(terpy)_2}^+$ and $\mathrm{O_2}$ react was determined at the conditions of the kinetic experiments: $[\mathrm{Cu}^+]$, 4.7×10^{-5} to 5.6×10^{-4} *M*; [terpy], 2.0×10^{-3} *M*; $[\mathrm{CH_3CN}]$, 3.5 *M*; pH 7.1. The mean value obtained from eight independent determinations of the ratio of the number of moles copper(I) oxidized per mole of $\mathrm{O_2}$ consumed, $\mathrm{Cu^+{:}O_2}$, is 2.11 ± 0.07. We also observe that product spectra resulting from the oxidation of $\mathrm{Cu(terpy)_2}^+$ by $\mathrm{O_2}$ corresponds to complete conversion to $\mathrm{Cu(terpy)_2}^{2+}$, as determined by comparison with a spectrum of an authentic Cu^{2+} solution containing terpy and $\mathrm{CH_3CN}$ under identical conditions. These two facts indicate that the reaction studied kinetically is that shown in eq 3. In

$$2\mathrm{Cu(terpy)_2}^+ + \mathrm{O_2} \xrightarrow{\mathrm{H^+}} 2\mathrm{Cu(terpy)_2}^{2+} + \mathrm{H_2O_2} \qquad (3)$$

particular, under the reaction conditions employed in this study any secondary reactions of $\mathrm{H_2O_2}$ with $\mathrm{Cu(terpy)_2}^+$ and/or $\mathrm{Cu(terpy)_2}^{2+}$ are not important.

Kinetics. The method of initial rates was used to determine the order of reaction 3 with respect to $\mathrm{Cu(terpy)_2}^+$ and $\mathrm{O_2}$. These results are presented in Figure 3. Slopes of 1.04 ± 0.02 and 0.92 ± 0.06 for the initial rate dependence on Cu^+ and $\mathrm{O_2}$, respectively, clearly show that the reactions are first order in both copper and oxygen over the concentration ranges studied. Further support for a second-order reaction overall is obtained from the fact that data obtained at fixed terpy and $\mathrm{CH_3CN}$ concentrations fit the integrated second-order rate equation, eq 2.

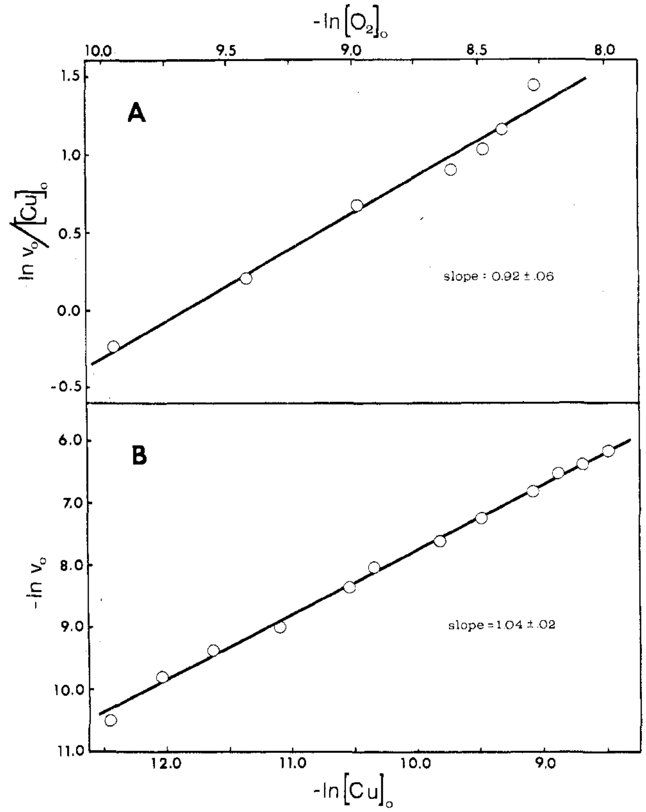

Figure 3. Initial rate, ν_0, of the oxidation of $\mathrm{Cu(terpy)_2}^+$ by $\mathrm{O_2}$. Each data symbol represents the mean value and standard deviation of the mean of two to five replicate experiments. The straight line represents a linear least-squares fit of the data. A: $\ln (\nu_0/[\mathrm{Cu}^+]_0)$ as a function of ln (initial $\mathrm{O_2}$ concentration), $\ln [\mathrm{O_2}]_0$. Conditions: $[\mathrm{Cu}^+] = 2.17 \times 10^{-4}$–$2.00 \times 10^{-5}$ *M*, [terpy] = 1.5×10^{-3} *M*, $[\mathrm{CH_3CN}] = 3.5$ *M*, pH 7.1, $I = 0.2$, 25.0°. B: $\ln \nu_0$ as a function of ln (initial Cu^+ concentration), $\ln [\mathrm{Cu}^+]_0$. Conditions: [terpy] = 1.5×10^{-3} *M*, $[\mathrm{CH_3CN}] = 3.5$ *M*, pH 7.1, $I = 0.2$, 25.0°.

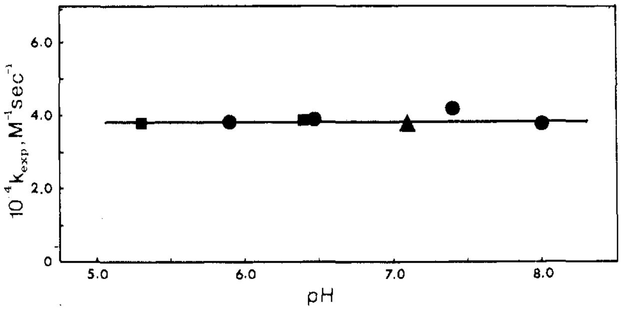

Figure 4. Observed second-order rate constant, k_{exptl}, as a function of pH. Data symbols represent the mean and standard deviations of duplicate experiments: ●, phosphate buffer, $[\mathrm{Cu}^+] = 2.0 \times 10^{-4}$ *M*, [terpy] = 1.5×10^{-3} *M*, $[\mathrm{CH_3CN}] = 3.5$ *M*, $I = 0.2$, 25.0°; ■, same conditions using acetate buffer; ▲, phosphate buffer, $[\mathrm{Cu}^+] = 1.68 \times 10^{-4}$ *M*, [terpy] = 1.5×10^{-3} *M*, $[\mathrm{CH_3CN}] = 3.5$ *M*, $I = 0.2$, 25°.

Figure 4 shows data representing the influence of pH on the second-order rate constant. Two observations can be made concerning these data. First, the rate is independent of pH over the range 5.3–8.0. Below pH 5.3 appreciable protonation of terpy occurs, thus complicating the interpretation of any pH effects in this region (see below); above pH 8.0 hydrolysis occurs. Second, the rate is independent of the identity of the buffering system (phosphate and acetate). Indeed, data obtained in the absence of a buffer fall on the line shown in Figure 4.

The second-order rate constant, k_{exptl}, was found to be dependent on the concentrations of $\mathrm{CH_3CN}$ and excess terpy, where excess terpy, $[\mathrm{terpy}]_{\mathrm{xs}}$, is defined as $[\mathrm{terpy}]_{\mathrm{tot}} - 2[\mathrm{Cu}^+]_0$,

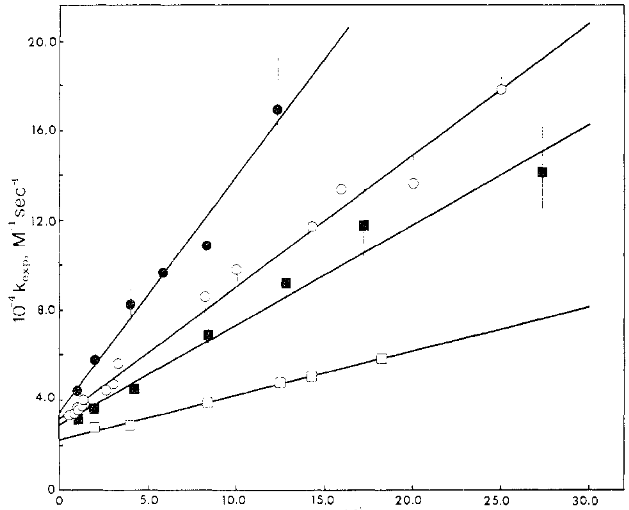

Figure 5. Observed second-order rate constant, k_{exptl}, as a function of reciprocal excess terpy concentration, $[\text{terpy}]_{\text{xs}}^{-1}$, at four different fixed CH_3CN concentrations (see text and eq 4). Each data point represents the mean value of two to six replicate experiments. Data symbols and error bars represent standard deviations of the mean. The straight lines represent a linear least-squares fit of the data for each CH_3CN concentration. All data were collected at 25.0°, $I = 0.2$, pH 7.1: □, $[CH_3CN] = 2.0\,M$, $[Cu^+] = 4.00 \times 10^{-5}\,M$, $[\text{terpy}] = 1.20 \times 10^{-4}$–$5.80 \times 10^{-4}\,M$; ■, $[CH_3CN] = 2.8\,M$, $[Cu^+] = 3.94 \times 10^{-5}$–$4.17 \times 10^{-5}\,M$, $[\text{terpy}] = 1.20 \times 10^{-4}$–$11.2 \times 10^{-4}\,M$. ○, $[CH_3CN] = 3.5\,M$, $[Cu^+] = 1.00 \times 10^{-5}$–$1.37 \times 10^{-4}\,M$, $[\text{terpy}] = 1.20 \times 10^{-4}$–$2.00 \times 10^{-3}\,M$. ●, $[CH_3CN] = 4.5\,M$, $[Cu^+] = 3.93 \times 10^{-5}\,M$, $[\text{terpy}] = 1.60 \times 10^{-4}$–$1.10 \times 10^{-3}\,M$.

Table I. Linear Least-Squares Analysis of Rate Data Presented in Figure 5[a]

$[CH_3CN]$, M	Intercept × 10^{-4}, M^{-1} sec^{-1}	Slope, sec^{-1}	10(slope)/$[CH_3CN]^2$,[b] M^{-2} sec^{-1}
2.0	2.26 ± 0.08	1.95 ± 0.07	4.9 ± 0.2
2.8	2.96 ± 0.44	4.44 ± 0.32	5.7 ± 0.4
3.5	3.16 ± 0.14	5.90 ± 0.16	4.8 ± 0.1
4.5	3.52 ± 0.62	10.48 ± 0.92	5.2 ± 0.5

[a] The uncertainties represent one standard deviation in the least-squares fit of the data to eq 4. [b] Mean (slope)/$[CH_3CN]^2$ = 5.1 (±0.4) × 10^{-1} M^{-2} sec^{-1}.

and $[Cu^+]_0$ is the initial Cu^+ concentration. The data presented in Figures 5 and 6 indicate that k_{exptl} can be expressed as a function of CH_3CN and terpy as shown in eq 4,

$$k_{\text{exptl}} = a + b[CH_3CN] + \frac{c[CH_3CN]^2}{[\text{terpy}]_{\text{xs}}} \tag{4}$$

where $a = 1.6\ (\pm 0.2) \times 10^4\ M^{-1}$ sec^{-1}, $b = 4.8\ (\pm 0.9) \times 10^3\ M^{-2}$ sec^{-1}, and $c = 5.1\ (\pm 0.4) \times 10^{-1}\ M^{-2}$ sec^{-1}.

Figure 5 shows a linear relationship between k_{exptl} and $[\text{terpy}]_{\text{xs}}^{-1}$ at four different CH_3CN concentrations, as required by eq 4. According to eq 4, the slope of each line in Figure 5 divided by $[CH_3CN]^2$ should take on the same value c for each of the CH_3CN concentrations investigated. Table I is a tablulation of the slopes and intercepts from Figure 5 as determined by a linear least-squares fit of the data. Column 4 indicates that at all CH_3CN concentrations investigated, the linear least-squares slopes divided by the square of the CH_3CN concentrations assume a constant value within the limits of experimental error. The mean value is

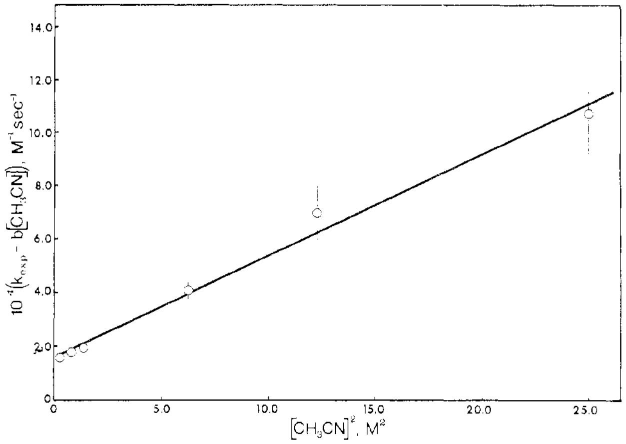

Figure 6. Plot of $k_{\text{exptl}} - b[CH_3CN]$ (see text and eq 4) as a function of $[CH_3CN]^2$ at a fixed excess terpy concentration. Each data point represents the mean value of two to five replicate experiments. Data symbols and error bars represent standard deviations of the mean. The straight line represents a linear least-squares fit of the data. Conditions: $[\text{terpy}]_{\text{xs}} = 1.25 \times 10^{-4}\,M$, $[Cu^{2+}] = 3.53 \times 10^{-5}$–$4.03 \times 10^{-5}\,M$, pH 7.1, $I = 0.2$, 25.0°.

$$(\text{slope})/[CH_3CN]^2 = 5.1\ (\pm 0.4) \times 10^{-1}\ M^{-2}\ \text{sec}^{-1}$$

The data presented in Table I show that the intercepts in Figure 5 are linearly dependent on the CH_3CN concentration according to eq 5, where $a = 1.43\ (\pm 0.31) \times 10^4\ M^{-1}$ sec^{-1}

$$\text{intercept} = a + b[CH_3CN] \tag{5}$$

and $b = 4.84\ (\pm 0.94) \times 10^3\ M^{-2}$ sec^{-1}. This linear dependence on $[CH_3CN]$ is also required by eq 4.

By rearranging eq 4, it can be seen that a plot of $k_{\text{exptl}} - b[CH_3CN]$ as a function of $[CH_3CN]^2$ should yield a straight line at a constant value of $[\text{terpy}]_{\text{xs}}$. Such a plot is shown in Figure 6 where the value for the constant b was obtained as shown in the previous paragraph. The product of the linear least-squares slope of Figure 6 (3.78 (±0.20) × $10^3\ M^{-3}$ sec^{-1}) and the excess terpy concentration (1.25 × 10^{-4} M), slope × $[\text{terpy}]_{\text{xs}}$, is 4.5 (±0.2) × $10^{-1}\ M^{-2}$ sec^{-1}. This is the same, within the limits of experimental error, as the mean value of (slope)/$[CH_3CN]^2$ obtained from Figure 5 and listed in Table I. This agreement is required according to eq 4.

The intercept in Figure 6, which represents the second-order rate constant at zero CH_3CN concentration, is 1.60 (±0.22) × $10^4\ M^{-1}$ sec^{-1}. This agrees, within the limits of experimental error, with the value 1.43 (±0.31) × $10^4\ M^{-1}$ sec^{-1} that one obtains from extrapolating the intercept data from Figure 5 to zero CH_3CN concentration (a in eq 5).

Thus the analytical expression for k_{exptl} in eq 4 adequately describes all of the kinetic data presented in Figures 4–6. The temperature dependence of k_{exptl} was determined over the range from 298 to 275°K when $[Cu^+] = 1.17 \times 10^{-4}\,M$, $[\text{terpy}] = 1.5 \times 10^{-3}\,M$, $[CH_3CN] = 3.5\,M$, pH is 6.9, and $I = 0.2\,M$. The calculated activation energy, E_a, is 8.1 (±0.3) kcal.

Discussion

The experimental rate law shown in eq 4 is consistent with

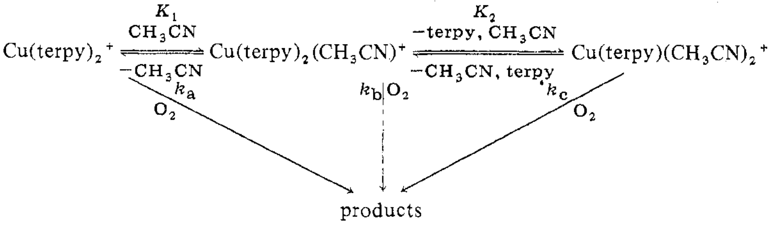
$$\mathrm{Cu(terpy)_2^+} \underset{-\mathrm{CH_3CN}}{\overset{K_1 \atop \mathrm{CH_3CN}}{\rightleftharpoons}} \mathrm{Cu(terpy)_2(CH_3CN)^+} \underset{-\mathrm{CH_3CN},\ \mathrm{terpy}}{\overset{K_2 \atop -\mathrm{terpy},\ \mathrm{CH_3CN}}{\rightleftharpoons}} \mathrm{Cu(terpy)(CH_3CN)_2^+} \tag{6}$$

the proposed reaction scheme of eq 6. Considering each of the three pathways to product formation independently, the rate law for path a can be expressed as in eq 7.

$$\text{rate} = k_a[\text{Cu(terpy)}_2{}^+][\text{O}_2] \qquad (7)$$

The rate law for path b is

$$\text{rate} = k_b[\text{Cu(terpy)}_2(\text{CH}_3\text{CN})^+][\text{O}_2]$$

If we assume that K_1 and K_2 are rapidly established equilibria and that the concentration of $\text{Cu(terpy)}_2(\text{CH}_3\text{CN})^+$ is determined by the K_1 equilibrium, then the rate law for path b can be expressed in terms of $\text{Cu(terpy)}_2{}^+$

$$[\text{Cu(terpy)}_2(\text{CH}_3\text{CN})^+] = K_1[\text{Cu(terpy)}_2{}^+][\text{CH}_3\text{CN}]$$

$$\text{rate} = k_bK_1[\text{CH}_3\text{CN}][\text{Cu(terpy)}_2{}^+][\text{O}_2] \qquad (8)$$

The assumption that K_1 and K_2 are rapidly established equilibria is valid since copper(I) is a labile d^{10} system. The assumption that the K_1 equilibrium alone determines the concentration of $\text{Cu(terpy)}_2(\text{CH}_3\text{CN})^+$ appears to be justified since, according to the continuous-variations plot shown in Figure 1, K_2 must be small. In addition, these kinetic experiments were carried out in the presence of excess terpy which would favor formation of the bis(terpyridine) complex.

The rate law for path c is given as

$$\text{rate} = k_c[\text{Cu(terpy)}(\text{CH}_3\text{CN})_2{}^+][\text{O}_2]$$

Assuming K_1 and K_2 to be rapidly established equilibria, the rate law for this path can also be expressed in terms of $\text{Cu(terpy)}_2{}^+$

$$[\text{Cu(terpy)}(\text{CH}_3\text{CN})_2{}^+] = K_1K_2\frac{[\text{Cu(terpy)}_2{}^+][\text{CH}_3\text{CN}]^2}{[\text{terpy}]}$$

$$\text{rate} = \frac{k_cK_1K_2[\text{CH}_3\text{CN}]^2}{[\text{terpy}]}[\text{Cu(terpy)}_2{}^+][\text{O}_2] \qquad (9)$$

The overall rate of disappearance of $\text{Cu(terpy)}_2{}^+$ is then the sum of eq 7–9 as shown in eq 10. This is consistent with eq

$$\text{rate} = \left(k_a + k_bK_1[\text{CH}_3\text{CN}] + \frac{k_cK_1K_2[\text{CH}_3\text{CN}]^2}{[\text{terpy}]}\right)[\text{Cu(terpy)}_2{}^+][\text{O}_2] \qquad (10)$$

4 where $a = k_a$, $b = k_bK_1$, and $c = k_cK_1K_2$.

Path a involves the second-order oxidation of $\text{Cu(terpy)}_2{}^+$ by O_2. There are three possibilities concerning the mode of activation for this step. The most likely possibility is the direct formation of a copper–oxygen bond, thus increasing the coordination number on going to the transition state. This could be considered as an inner-sphere redox process. Zuberbühler has studied the autoxidation of several cuprous complexes where the rates of oxidation increase with increasing free ligand concentration, suggesting that the coordination number of the copper increases on going to the rate-determining step.[6,8] Pentacoordinate copper(I) is a relatively stable configuration, and the copper(II) product, $\text{Cu(terpy)}_2{}^{2+}$, has been shown to be hexacoordinate (see above). Another possibility not involving an increase in coordination number is terpy ring opening followed by direct formation of a copper–oxygen bond. This should be a facile process for a d^{10} ion. A third possibility is oxidation without the direct formation of a copper–oxygen bond, presumably with electron transfer occurring through the π-electron system of the terpy ligand.

It is not clear whether path b represents oxidation of a pentacoordinate $\text{Cu(terpy)}_2(\text{CH}_3\text{CN})^+$ ion or a tetracoordinate complex formed by the opening of a terpy chelate ring. Direct formation of a copper–oxygen bond seems probable here also, but one cannot rule out the possibility of electron transfer through the terpy π-electron system. There also exists the possibility that path b represents an CH_3CN solvation effect on the oxidation of $\text{Cu(terpy)}_2{}^+$, i.e., that CH_3CN does not form a bond to copper in the first coordination shell. While this possibility cannot be completely ruled out, one should bear in mind that $\text{Cu(terpy)}_2(\text{CH}_3\text{CN})^+$ can be viewed as a species intermediate to $\text{Cu(terpy)}_2{}^+$ and $\text{Cu(terpy)}(\text{CH}_3\text{CN})_2{}^+$, and consequently its existence in solution is not unreasonable.

Path c provides the same choices between inner- and outer-sphere redox as paths a and b. The most likely possibility, however, is the direct attack of O_2 on the tetracoordinate copper(I) ion to form a pentacoordinate transition state leading to products. It is noteworthy that while the species $\text{Cu}(\text{CH}_3\text{CN})_2{}^+$ is inert to air oxidation,[4] the mixed complex $\text{Cu(terpy)}(\text{CH}_3\text{CN})_2{}^+$ is oxidized by O_2.

There also exists the question in each of the above reaction paths leading to the reduction of O_2 to H_2O_2 as to whether this reduction occurs as two one-electron steps or as a single two-electron step. Let CuL^+ represent $\text{Cu(terpy)}_2{}^+$, $\text{Cu(terpy)}_2(\text{CH}_3\text{CN})^+$, or $\text{Cu(terpy)}(\text{CH}_3\text{CN})_2{}^+$ in the following discussion.

A three-step mechanism involving a simultaneous two-electron reduction of O_2 to give H_2O_2 directly is

$$\text{CuL}^+ + \text{O}_2 \underset{k_{-11}}{\overset{k_{11}}{\rightleftharpoons}} \text{CuLO}_2{}^+ \qquad (11)$$

$$\text{CuLO}_2{}^+ + \text{CuL}^+ \xrightarrow{k_{12}} 2\text{CuL}^{2+} + \text{O}_2{}^{2-} \qquad (12)$$

$$\text{O}_2{}^{2-} + 2\text{H}^+ \rightarrow \text{H}_2\text{O}_2 \qquad (13)$$

When eq 12 is rate determining and the steady-state assumption is applied to the concentration of the intermediate $\text{CuLO}_2{}^+$, rate expression 14 is obtained. Under the conditions

$$\text{rate} = \frac{k_{11}k_{12}[\text{CuL}^+]^2[\text{O}_2]}{k_{-11} + k_{12}[\text{CuL}^+]} \qquad (14)$$

where $k_{-11} >> k_{12}[\text{CuL}^+]$, eq 14 reduces to eq 15 and

$$\text{rate} = \frac{k_{11}k_{12}[\text{CuL}^+]^2[\text{O}_2]}{k_{-11}} \qquad (15)$$

second-order dependence on CuL^+ would be observed. Such second-order dependence would suggest a simultaneous two-electron reduction of O_2 to yield H_2O_2 directly. However, under those conditions where $k_{12}[\text{CuL}^+] >> k_{-11}$ eq 14 reduces to eq 16 which exhibits first-order dependence on $[\text{CuL}^+]$.

$$\text{rate} = k_{11}[\text{CuL}^+][\text{O}_2] \qquad (16)$$

This is of the same form as eq 1 observed in this study at fixed terpy and CH_3CN concentrations.

An alternative mechanism involving a stepwise reduction of O_2 is

$$\text{CuL}^+ + \text{O}_2 \xrightarrow{k_{17}} \text{CuL}^{2+} + \text{O}_2{}^- \qquad (17)$$

$$\text{O}_2{}^- + \text{H}^+ \rightarrow \text{HO}_2 \qquad (18)$$

$$\text{CuL}^+ + \text{HO}_2 \rightarrow \text{CuL}^{2+} + \text{HO}_2{}^- \qquad (19)$$

$$\text{HO}_2{}^- + \text{H}^+ \rightarrow \text{H}_2\text{O}_2 \qquad (20)$$

If eq 17 represents the rate-determining step, then the rate law for this mechanism is

$$\text{rate} = k_{17}[\text{CuL}^+][\text{O}_2] \qquad (21)$$

which is also consistent with our observed rate law given in eq 1.

Our results then are consistent with both a stepwise one-electron reduction of O_2 and a simultaneous two-electron reduction of O_2 under those conditions where $k_{12}[\text{CuL}^+] >> k_{-11}$. A deviation of the rate law from first-order dependence on $[\text{CuL}^+]$ could be taken as evidence supporting a simultaneous two-electron-transfer mechanism. Figure 3 shows that

Table II. Second-Order Rate Constants for the Oxidation of Various Cuprous Complexes by Molecular Oxygen

Complex	k, M^{-1} sec^{-1}	Ref
Cu_{aq}^+	7.0×10^4	*a, e*
$Cu(NH_3)_2^+$	3.6×10	*b, f*
$Cu(imid)_2$	2.8×10	*b, f, h*
$Cu(Me(imid))_2^+$	2.2×10^2	*b, f, i*
$Cu(Hi)^+$	5.2×10^4	*c, f, j*
$Cu(HiH)_2^{3+}$	2.3×10^3	*c, f, k*
$Cu(His)$	9.0×10^4	*c, f, l*
$Cu(HisH)_2^+$	2.0×10^3	*c, f, m*
$Cu(bipy)_2^+$	6.5×10^3	*d, g*
$Cu(terpy)_2^+$	1.6×10^4	This work

[a] A. Zuberbühler, *Helv. Chim. Acta*, **53**, 473 (1970). [b] A. Zuberbühler, *Chimia*, **23**, 416 (1969). [c] A. Zuberbühler, *Helv. Chim. Acta*, **53**, 669 (1970). [d] I. Pecht and M. Anbar, *J. Chem. Soc. A*, 1902 (1968). [e] At 20°, pH >3, $I = 0.2$. [f] At 20°, $I = 0.2$. [g] At 25°. [h] imid = imidazole. [i] Me(imid) = *N*-methylimidazole. [j] Hi = histamine. [k] HiH = monoprotonated histamine. [l] His = histidine monoanion. [m] HisH = histidine.

first-order dependence on $[CuL^+]$ was observed even at very low CuL^+ concentration, where according to eq 14 and 15 deviations from first-order behavior would be most likely to be observed.

From thermodynamic considerations, one might expect the reaction to proceed via a simultaneous two-electron reduction of O_2. While reduction potentials for the complexes CuL^+ being discussed here are not available in acetonitrile–water solvent mixtures, one can obtain some useful information from the Cu^{2+}–Cu^+ aqueous ($E° = 0.15$ V)[18] and 2,2′-bipyridine ($E^* = 0.12$ V)[19] couples. When these are considered with the O_2–HO_2 couple ($E° = -0.10$ or -0.32 V)[20,21] and HO_2–H_2O_2 couple ($E° = 1.40$ V),[20] we see that the first step of the stepwise reduction of O_2 by Cu_{aq}^+ or $Cu(bipy)_2^+$ is thermodynamically unfavorable, the driving force for the reaction being the second one-electron transfer. The O_2–H_2O_2 couple ($E° = 0.67$),[21] however, provides a thermodynamically favorable simultaneous two-electron redox path. These thermodynamic considerations are probably also true in a relative sense for the terpy system reported here. It should be noted, however, that strict first-order dependence on $[Cu^+(aq)]$[4] and $[Cu(bipy)_2^+]$[9] have been reported for the reduction of O_2 by Cu_{aq}^+ and $Cu(bipy)_2^+$, respectively. In fact, the only kinetic evidence for the thermodynamically favored simultaneous two-electron reduction of O_2 by a cuprous complex is the autoxidation of cuprous chloride in glacial acetic acid, which exhibits second-order $[Cu^+]$ dependence on the rate.[22]

We must conclude then that our kinetic results are unable to distinguish between a simultaneous two-electron and stepwise one-electron reduction of O_2. On the basis of thermodynamic considerations, however, one might favor the simultaneous two-electron reduction, in which case the condition $k_{12}[CuL^+] >> k_{-11}$ must obtain even at the low cuprous concentrations shown in Figure 3.

Table II summarizes available rate data for the autoxidation of cuprous complexes containing nitrogen donor ligands. While these data were collected under differing experimental conditions, there appears to be little variation in the second-order rate constants except for $Cu(NH_3)_2^+$, $Cu(imidazole)_2^+$, and $Cu(N\text{-methylimidazole})_2^+$. These systems were found to have a more effecient ligand-dependent path with third-order rate constants of 3.2×10^4, 1.1×10^4, and 3.6×10^4 M^{-2} sec^{-1} for the NH_3, imidazole, and *N*-methylimidazole systems, respectively.[6] This suggests that, in these systems at least, the energetically favorable path to products may involve a four-coordinate transition state. This would tend to support terpy ring opening prior to reaction with O_2 in the $Cu(terpy)_2^+$ system reported here.

Activation parameters are not available for the complexes listed in Table II. Gray reported an E_a of 8.4 kcal for the oxidation of Cu_{aq}^+ by O_2 in aqueous acetonitrile. This is similar to 8.1 kcal reported here as a composite value for paths a, b, and c in the $Cu(terpy)_2^+$ system.

According to reaction scheme 6, the value for a in eq 4 (1.6×10^4 M^{-1} sec^{-1}) can be taken as the second-order rate constant for the rate of oxidation of $Cu(terpy)_2^+$ by O_2 in aqueous solution. This result is consistent with the data listed in Table II. James and Williams[19] have investigated the variation in Cu^{2+}–Cu^+ redox potentials for complexes of substituted bipy and phen.[10] They reported that an increase in σ-donor strength stabilizes the cupric state and an increase in π-acceptor strength stabilizes the cuprous state. The pK_a values for terpy and bipy (4.69 and 4.50, respectively) suggest that both have comparable σ-donor strengths.[19] The π-acceptor ability of terpy acting as a bidentate ligand with one pyridine ring freely rotating in solution (see Results) should be similar to that of bipy. The similarity of the autoxidation rate constants of $Cu(bipy)_2^+$ and $Cu(terpy)_2^+$ shown in Table II then suggests that the energy of the transition state is not appreciably influenced by the presence of a third pyridine ring in terpy; i.e., the formation of a new copper–nitrogen bond on going from reactants to products does not significantly influence the rate of oxidation of $Cu(terpy)_2^+$. However, this need not necessarily be the case for the mono complex, $Cu(terpy)(CH_3CN)_2^+$, and may explain why a reaction path involving the corresponding mono(bipyridine) complex was not observed.[9]

Acknowledgment. We wish to thank L. J. Gestaut for helpful discussions concerning the computer programs used in this study. Acknowledgment is made to the donors of the Petroleum Research Fund, administered by the American Chemical Society, for support of this research. Support from a Biomedical Sciences Support Grant, administered by Duke University, and the Duke University Research Council is also acknowledged.

Registry No. I, 54688-84-5.

References and Notes

(1) NSF Undergraduate Research Participation Program Fellow.
(2) For a recent review see R. Lontie and R. Witters in "Inorganic Biochemistry", Vol. I, G. L. Eichhorn, Ed., Elsevier, New York, N.Y., 1973, Chapter 12.
(3) H. Nord, *Acta Chem. Scand.*, **9**, 430 (1955).
(4) R. D. Gray, *J. Am. Chem. Soc.*, **91**, 56 (1969).
(5) A. Zuberbühler, *Helv. Chim. Acta*, **53**, 473 (1970).
(6) A. Zuberbühler, *Chimia*, **23**, 416 (1969).
(7) A. Zuberbühler, *Helv. Chim. Acta*, **50**, 466 (1967).
(8) A. Zuberbühler, *Helv. Chim. Acta*, **53**, 669 (1970).
(9) I. Pecht and M. Anbar, *J. Chem. Soc. A*, 1902 (1968).
(10) Abbreviations used in this paper are as follows: 2,2′,2″-terpyridine, terpy; 2,2′-bipyridine, bipy; 1,10-phenanthroline, phen.
(11) B. J. Hathaway, D. G. Holah, and J. D. Postlethwaite, *J. Chem. Soc.*, 3215 (1961).
(12) P. Hemmerich and C. Sigwart, *Experientia*, **19**, 488 (1963).
(13) D. F. Shriver, "The Manipulation of Air-Sensitive Compounds", McGraw-Hill, New York, N.Y., 1969, p 92.
(14) P. Job, *C. R. Hebd. Seances. Acad. Sci.*, **180**, 938 (1925).
(15) K. Nakamoto, *J. Phys. Chem.*, **64**, 1420 (1960).
(16) "Beckman 96260 Oxygen Adaptor Instruction Manual", Beckman Instrument Co., Fullerton, Calif., p 11; data obtained from "Standard Methods for the Examination of Water", American Public Health Association.
(17) R. Hogg and R. G. Wilkins, *J. Chem. Soc.*, 341 (1962).
(18) W. M. Latimer, "The Oxidation States of the Elements and Their Potential in Aqueous Solution", 2nd ed, Prentice-Hall, New York, N.Y., 1952, p 240.
(19) B. R. James and R. J. P. Williams, *J. Chem. Soc.*, 2007 (1961). E^* as defined by James and Williams refers to the measured potential in aqueous solution when the degrees of formation of the $(bipy)_2$ complexes of Cu^+ and Cu^{2+} are equal. While this differs from the conventionally defined redox potential, its use here to predict reaction paths which are thermodynamically relatively favorable or unfavorable is probably justified.
(20) H. Taube, *J. Gen. Physiol.*, **49**, (No. 1, part 2), 29 (1965).
(21) P. George in "Oxidases and Related Redox Systems," Vol. I, T. E. King, H. S. Mason, and M. Morrison, Ed., Wiley, New York, N.Y., 1965, p 3.
(22) P. M. Henry, *Inorg. Chem.*, **5**, 688 (1966).